RESEARCH

Can Sonoelastography and Multiphasic Computed Tomography be used to Differentiate RCC Subtypes?

Suat Keskin[1], Merter Keçeli[2]

[1] Department of Radiology, KTO Karatay Univercity Medical School, Konya, Turkey
[2] Department of Radiology, Konya City Hospital, Konya, Turkey

ORCID; 0000-0001-9204-3961, 0000-0002-9412-6733

Abstract: The aim of this study is to investigate if any correlation exists between strain elastography (SE) and multiphasic computed tomography (CT) findings in Renal Cell Carcinoma (RCC) subtypes. This study investigated any correlation existed between the SE findings and the tCT density values based on phase for the RCC subtypes. The SE and CT was performed on 43 patients prospectively. The RCC were classified according to histological subtypes. The strain indexes (SI) and mean density measurements of the CT were calculated. The mean age of the patients is 57.4 (35-81) years. A positive significant correlation was detected between the renal parenchyma SE and the renal mass SE values in the clear cell RCC subtype (p=0.004). Negative significant correlation was found between the renal mass SE and SI in the papillary subtype (p=0.047). A negative significant correlation was detected between the renal mass SE and the density values on the nonenhanced phase CT in males (p=0.019). There is no significant correlation between SE values and density values obtained from the corticomedullary, nephrographic and excretory CT phases. Significant correlation between the density values obtained in the nonenhanced phase CT and the SE values was detected based on gender. It was seen that the SI values calculated by evaluating the RCC mass with SE would be useful in subtype distinction.

INTRODUCTION

Renal cell carcinoma (RCC) constitutes approximately 2% of all cancer types, worldwide[1]. Recently, thanks to improvements in medical imaging methods, there has been an increase in the ability to detect renal cell carcinomas incidentally[2]. The most common subtypes of RCC are clear cell, chromophobe, and papillary carcinomas[3]. Each of the subtypes has a different prognosis. It has been reported that the clear cell subtype has the worst prognosis. Compared to other subtypes, clear cell RCC has a lower five-year survival rate and a higher likelihood of metastasis[4]. Different radiologic methods, such as ultrasonography (US) and computed tomography (CT), are performed to image and diagnose RCC[5]. US elastography is a radiologic modality that has begun to be used to diagnose carcinomas. With the help of this method, the tissue stiffness ratio can be revealed in real-time on conventional B-mode images. In the literature, some studies have shown that malignant tissues are stiffer than benign tissues and this technique is effective in differentiating benign tissues from malignant tissues[6,7]. The other radiologic modality that is used to diagnose RCC is multiphasic CT. RCC subtypes can have different enhancement patterns on dynamic examination. For example, the clear cell RCC subtype has higher vascularization than the papillary subtype[8]. There is no study in the literature that examines if any correlation exists between the SE findings, which are obtained using elastography and mass enhancement patterns based on phase, and the findings that are obtained by multiphasic CT for RCC subtypes.

The aim of this study is to investigate if any correlation exists between the strain elastography (SE) findings and multiphasic CT enhancement patterns in RCC subtypes.

MATERIALS and METHODS

Study population

The study group comprised of 26 males and 17 females (total 43 patients) who underwent US imaging of a renal mass, including SE and multiphasic CT, at the authors' institution between March 2012 and August 2013. The decision of the ethics committee was obtained. Signed consent form was received from the participants. The mean age of the population was 57.4 ± 12.7 (range: 35-81 years). The diagnosis was made by pathological study after total resection. The histological subtype was found to be clear cell carcinoma in 32 patients, chromophobe cell carcinoma in 5 patients, and papillary cell carcinoma in 6 patients.

Received :04.06.2021
Received in revised form :28.07.2021
Accepted :10.08.2021
Available online :15.09.2021

Keywords:

Strain elastography
Renal cell cancer
Multiphasic renal computed tomography

Corresponding Author:
Suat Keskin
E-mail; drsuatkeskin@yahoo.com
http://dx.doi.org/10.29228/jamp.51655

Int J Acad Med Pharm,
2021; 3 (3); 249-253

Equipment and scanning

Computed tomography

The multiphasic multidetector CT examinations were carried out by same radiologist, with twenty years of experience in CT. Whole patients were investigated using a 64-multi-detector CT scanner (Siemens SOMATOM Sensation 64, Erlangen, Germany) with the following scanning parameters: 1.5 mm slice thickness, 0.6 mm collimation, 100 kV and 135 mAs, 1.4 mm increment, a gantry rotation time of 0.33 s, and a pitch of 0.9. While the patient was in the supine position, and the area from the diaphragm to the end of the iliac bones was identified as the field of examination. A scout image was acquired. Whole patients obtained approximately 100 ml of nonionic contrast medium (Ultravist 300; Bayer Schering Pharma, Berlin, Germany). The contrast medium was applied with a catheter placed in the right antecubital vein. An automated injector executed the contrast at a flow rate of 5 mm/sec. After the starts of the injection, the scan was executed 20 seconds. Before the nonionic contrast medium was given, first, the unenhanced phase was obtained, and then the corticomedullary phase (40-55 seconds), the nephrographic phase (90-120 seconds), and the excretory phase (approximately 7-8 minutes) were acquired. In the nephrographic phase, lesion sizes were measured, and then in the unenhanced, corticomedullary, nephrographic, and excretory phases, the densities were measured respectively. Density measurements were made from circular ROIs with an area of 10 mm2 in three separate regions of the renal lesion. It was then calculated for renal mass attenuation as the average of these values (Fig. 1-4). While measuring the density of the lesion, cystic, calcified and necrotic areas within the lesion were avoided.

Strain elastography

Sonoelastography examinations were accomplished by one radiologist with twenty years of experience in conventional sonography and ten years of experience in elastography. A digital sonography scanner (Aplio XG; Toshiba Medical Systems, Tokyo, Japan) supplied with SE soft ware and a convex 2.5-5 MHz multifrequency transducer (Model PVT-375BT, Serial Number: FDA 11Y4472) was experienced the patients by same radiologist both B-mode and elastographic sonography in the supine and lateral decubitus position. During breath holding after deep inspiration, all evaluations were executed. A target lesion was identificated on a B-mode US image, and then SE was carried out using the same probe. The probe was removed to compact manually and release the underlying tissue. During the sonoelastography, both the B-mode and elastographic images were exhibited as a two-panel image at the same time. When determining the elastographic pattern, only the lesions' solid portions were assessed. The elastographic image was demonstrated over the B-mode image in a color scale: red indicated tissue that experienced the greatest strain and had the softest component and blue indicated tissue that experienced no strain and had the hardest component. Green indicated tissue that had average strain9. The elastographic region of interest (ROI) consisted of both the renal lesions and the normal surrounding tissue. If there is a cystic area within the lesion, it was noted. But only the lesion's solid portions were assessed when appraising the elastographic pattern. The static images except for those of the 43 patients who were previously diagnosed as RCC with CT were reviewed by one radiologist who was blinded to the pathologic findings and the final diagnoses. The strain rate was measured for all kidney lesions (B) by comparing the tumor (A) with the renal cortex. First, the ROI was placed in the renal cortex. Then, the ROI was situated in the renal mass. The elasticity values in the ROI placed over the stiffest areas on the elastography image for the renal cortex and the renal mass were noted by the radiologist. The strain elastography index (SI:B/A), which reflected the stiffness of the lesion, was then automatically calculated (Fig.2).

Statistical analysis

Using SPSS version 20.0 software (SPSS, Chicago, IL, USA), statistical analyses were completed, and the data were showed as the mean ± standard deviation. Normal distribution was analyzed with the Kolmogorov-Smirnov test, and using the Mann-Whitney U test was used for a comparison of the non-parametrically distributed variables, while the independent Student's t-test, the differences between the two groups were tested for normally distributed variables. While investigating the associations between normally/non-normally distributed and/or ordinal variables, the correlation coefficients and their significance were calculated using the Pearson's/Spearman's test. The differences between the categorical variables were determined by using the $\chi 2$- test. One-way analysis of variance was employed to compare lesion size and CT density surrounded by the RCC subtypes. Levene's test was employed to evaluate the homogeneity of the variances. The Mann-Whitney U test was performed to test the significance of the pair-wise differences using the Bonferroni correction to adjust for multiple comparisons. Kruskal-Wallis tests were conducted to compare the differences in the CT density and elastography findings among the pathological subtypes. Two-tailed P values of less than 0.05 were received as being statistically significant.

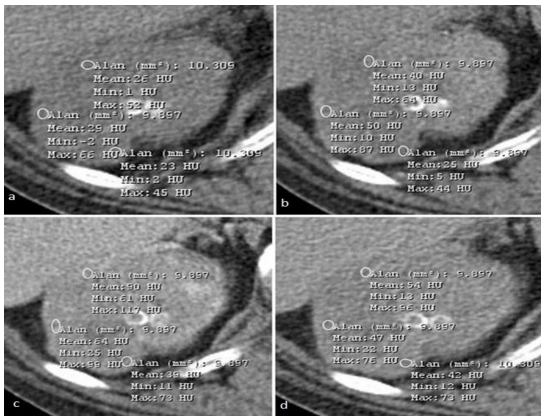

Figure 1. A 71-year-old man with clear cell carcinoma (arrows); standardized multidetector CT protocol for measuring mean tumor attenuation with three small 10 mm2 regions of interest in clear cell renal cell carcinoma. (a) Unenhanced phase; (b) Corticomedullary phase; (c) Nephrographic phase; and (d) Excretory phase.

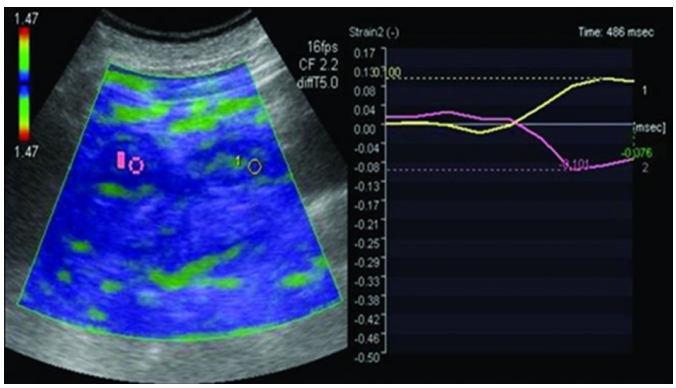

Figure 2. In order to calculate the strain index on an elastography image, the first region of interest (ROI) (A) was placed in the renal cortex. The second ROI (B) was plotted to the renal mass. The strain index was automatically calculated as an B / A

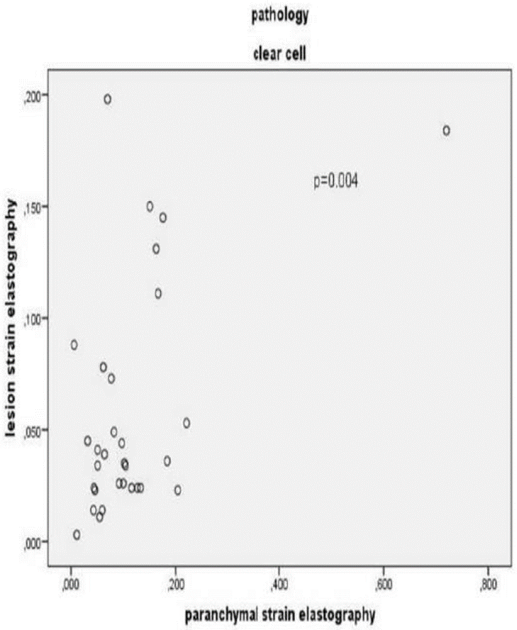

Figure 3. Punctate distribution graphic that reveals a positive significant correlation between the renal mass strain elastography values and the renal parenchymal strain elastography values in clear renal cell cancer

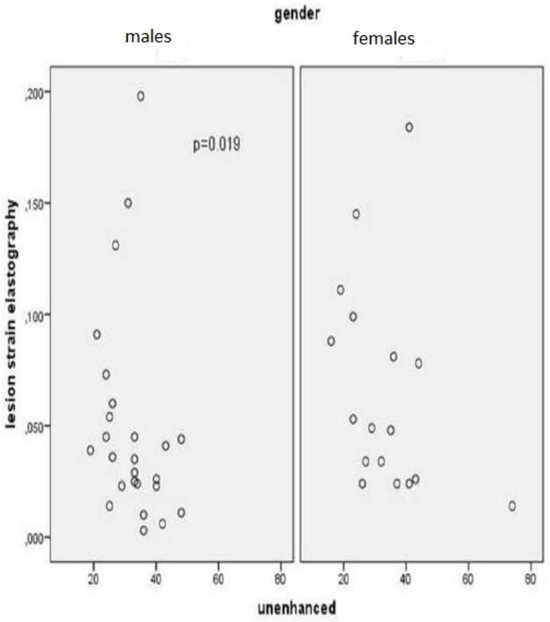

Figure 4. Punctate distribution graphic that reveals a negative significant correlation between the renal mass strain elastography values and the density values obtained in the nonenhanced phase in males

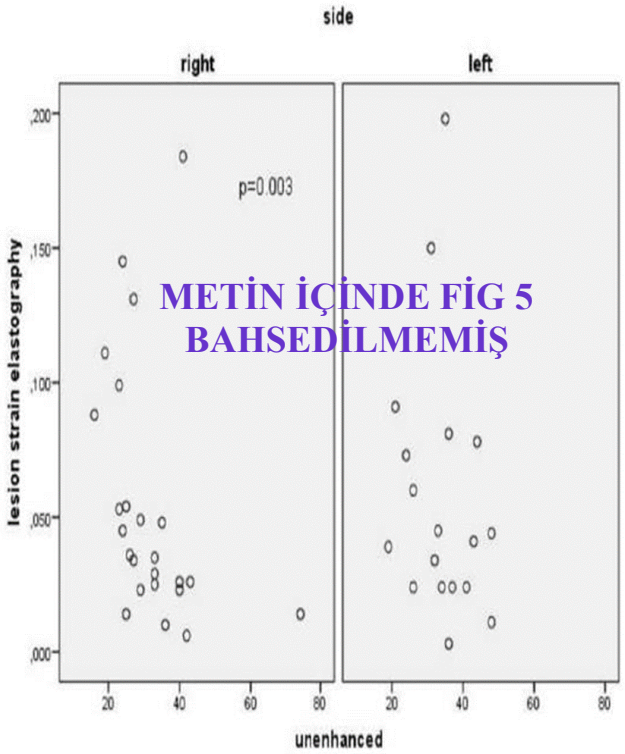

Figure 5. Punctate distribution graphic that reveals a negative significant correlation between the renal mass strain elastography values and the density values obtained in the nonenhanced phase in the right-sided masses

RESULTS

The obtained findings are summarized and the SE value and rate obtained from the renal parenchyma and RCC lesion are shown in Table.1. When the results are evaluated, a positive significant correlation was found between the renal parenchyma and the renal mass SE values and SI (respectively p=0.002 and p=0.004), There was statistically significant relationship between SE values and SE index and gender (respectively p=0,03 ve p=0,02). There was no significant correlation between SE values obtained from the renal mass and RCC subtypes (respectively p=0,62). The highest SI calculated from the renal mass was obtained in the Clear Cell Carcinoma subtype and the lowest SE was obtained in the Papillary RCC subtype. The highest SI mean value was found in Clear Cell RCC, the lowest SI mean value was found in the Papillary RCC subtype. In the Chromophobe RCC subtype, the SI mean value was among the values of the other two subtypes. Significant difference was found SI obtained from RCC subtypes lesions (p< 0.01)(Table.1).

There was statistical difference between RCC subtypes in lesion density measured in nonenhance CT (p=0.038). In the lesion densities obtained in multiphasic CT, the mean density in papillary type RCC was lower than the other subtypes and showed a difference (p=0.047). In Clear Cell and Papillary subtype RCC, the increase in lesion density that started in the corticomedullary phase increased further in the nephrographic phase. In the excretory phase, this density was decreasing. On the other hand, in Chromophobe RCC, the increasing lesion density in the corticomedullary phase decreased gradually in the following phases (Table 1).

Table 1. The mean and 95% CI of the CT densityin phases and elastography findings in the RCC subtypes

	Clear cell RCC		Chromophobe RCC		Papillary RCC	
	Mean	95% CI	Mean	95% CI	Mean	95% CI
Unenhanced (HU)	33,48±2,08	29,25-37,72	33,80±2,56	26,70-40,90	29±2,77	21,88-36,12
CM Phase (HU)	76,52±4,68	66,96-86,07	84,60±18,51	74,21-135,99	48,33±8,15	27,89-69,77
N Phase (HU)	83,84±3,57	76,55-91,13	69,40±8,56	45,64-93,16	63,67±10,02	37,91-89,42
Ex Phase (HU)	63,16±2,34	58,26-68,06	56,40±6,43	38,54-74,26	57,33±7,87	37,11-77,56
Prn SE (kPa)	0,12±0,02	0,07-0,16	0,07±0,02	0,01-0,13	0,08±0,02	0,01-0,14
Mass SE (kPa)	0,06±0,01	0,04-0,08	0,05±0,01	0,01-0,06	0,06±0,01	0,02-0,1
Lesion SI	3,29±0,37	2,53-4,06	2,32±0,82	0,04-4,59	1,98±0,81	0,11-4,07

RCC: Renal cell cancer; CI: Confidence interval; CT: Computed tomography, CM: corticomedullarry phase in enhanced CT, Nephrographyc phase, Ex: Excretion phase, Prn SE: paranchimal strain elastography values, Mass SE: Renal mass lesion strain elastography values, SI: Strain Index, HU: Hounsfield Unit, kPa: kiloPascal

When CT and elastography were compared, a high level of positive correlation was found between the SI obtained from renal masses and the HU values obtained from nonenhanced CT (p=0.03) (Figure 5).

DISCUSSION

The diagnosis of RCC can be made by sonographic mass identification. The multiphasic contrast CT is used for mass lesion characterization, showing the relationship with adjacent organs and vessels, and for retroperitoneal imaging. Sonographic elastography is a nonenhanced, easily performed technique that assesses the elasticity of tissues. This technique can be performed with qualitative, semiquantitative, and quantitative methods. Qualitative evaluation shows color coded images representing tissue stiffness with different colors. Semi-quantitative elastography shows color-coded imaging features of tissues. In this method, stress index values are calculated in response to the force induced in the tissues. Quantitative elastographic techniques such as acoustic radiation force impulse imaging measure the speed of shear waves generated from the force of acoustic radiation in tissues. It saves the calculated tissue hardness by converting it into numerical data.

The purpose of this study is to examine if there is significant correlation in RCC subtypes between SE and multiphasic CT findings. In the literature, some studies have investigated the density difference of RCC subtypes on multiphasic CT[10,11]. We could not find any other studies in the English-language medical literature comparing these two techniques in terms of differences between the RCC subtypes.

There are successful studies about intraabdominal tissue elastography in the literature[12-14]. Some of those studies have proven that sonoelastography could be useful for differentiating benign-malignant tissues, especially in the prostate and the liver[15,16]. Özkan et al, Orrlachio et al, Menzilcioğlu et al, Gao et al have conducted studies on renal fibrosis and renal transplant rejection in adult patients with the SE technique[17-20]. There are no studies on renal malignancy with this technique. Most studies were done with Shear Wave Elastography, Transtient Elastography and Acoustic Radiation Force Impulse Elastography techniques. One of the reasons why we use the SE technique, which is within our possibilities, is that it is cheaper and easier to obtain than other sonoelastography techniques. The SE values we obtained from renal masses are different according to the mentioned studies due to the technique used. The stiffness of the hard lesions is higher, thus the displacement and deformation is lower in SE technique. So, the strain of hard lesions is lower, but the SI of hard lesions is higher, because of the ratio[21]. There was no significant change in SI values among RCC subtypes. However, not many studies have investigated this subject for renal masses. Tan et al's study predicted that real time SE could be decisive in the differentiation of renal cell cancer and angiomyolipom[22]. Keskin et al's similar design study, in the distinction of RCC and AML diagnostic value of SI by grouping lesion size researched23. In this study, the mean SI value in RCC was 3.4 ± 0.3, 1.1 ± 0.1 calculated in AML. In this study, RCC was obtained close to these values in all subtypes. These results support the results of previous studies [23].

We did not find any study investigating whether there is any correlation between SE values and multiphase CT intensity values in RCC subtypes. In our study, we detected a significant correlation between the density values obtained in the nonenhanced phase, the renal mass SE values and the SI. We did not find a statistically significant relationship between the density values obtained in the corticomedullary, nephrographic and excretory stages and SE values.

Our study has some limitations. The first is that we have a small number of participants. The population participating in our study could not be homogenized. For example, RCC Clear Cell Carcinomas were more numerous than other subtypes. There was no sarcomatoid subtype among the RCCs included in the study. In addition, there are some limitations of the SE technique. Examination of deep tissue lesions with SE made it difficult to evaluate in obese patients due to the difficulty of external compression. To overcome this limitation, the following renal masses were excluded: masses that were too deep to localize and that could not be optimally compressed, especially masses that required intercostal level compression. It may not be possible to standardize the application of external compression among operators in SE. To eliminate this limitation, all SE examinations in our study were performed by a single experienced radiologist.

Conclusion

In our prospective study investigating the use of imaging techniques in the differential diagnosis of RCC subtypes, it was seen that the SI values calculated from the lesion would be useful. There was statistical difference between RCC subtypes in lesion density measured in nonenhanced CT. It has been concluded that two methods are useful in subtype discrimination due to the significant connection between nonenhanced CT and SI.

Conflict of Interest

The authors declare that they have no conflict of interest.

REFERENCES

1. Gore ME, Larkin JM. Challenges and opportunities for converting renal cell carcinoma into a chronic disease with targeted therapies. *Br J Cancer* 2011;104: 399–406.
2. Sun M, Thuret R, Abdollah F, Lughezzani G, Schmitges J, Tian Z, et al. Age-adjusted incidence, mortality, and survival rates of stage-specific renal cell carcinoma in North America: a trend analysis. *Eur Urol*. 2011 Jan;59(1):135-41.
3. Kovacs G, Akhtar M, Beckwith BJ, Bugert P, Cooper CS, Delahunt B, et al. The Heidelberg classification of renal cell tumours. *J Pathol*. 1997 Oct;183(2):131-3.
4. Cheville JC, Lohse CM, Zincke H, Weaver AL, Blute ML. Comparisons of outcome and prognostic features among histologic subtypes of renal cell carcinoma. *Am J Surg Pathol* 2003;27: 612–624.
5. Cho N, Jang M, Lyou CY, Park JS, Choi HY, Moon WK. Distinguishing benign from malignant masses at breast US: combined US elastography and color doppler US--influence on radiologist accuracy. *Radiology*. 2012 Jan;262(1):80-90.
6. Dumitriu D, Dudea S, Botar-Jid C, Baciut M, Baciut G. Real-time sonoelastography of major salivary gland tumors. *AJR Am J Roentgenol*. 2011 Nov;197(5):W924-30.
7. Jung HJ, Hahn SY, Choi HY, Park SH, Park HK. Breast sonographic elastography using an advanced breast tissue-specific imaging preset: initial clinical results. *J Ultrasound Med*. 2012 Feb;31(2):273-80.
8. Zhang J, Lefkowitz RA, Ishill NM, Wang L, Moskowitz CS, Russo P, et al. Solid renal cortical tumors: differentiation with CT. *Radiology*. 2007 Aug;244(2):494-504.
9. Itoh A, Ueno E, Tohno E, Kamma H, Takahashi H, Shiina T, et al. Breast disease: clinical application of US elastography for diagnosis. *Radiology*. 2006 May;239(2):341-50.
10. Jung SC, Cho JY, Kim SH. Subtype differentiation of small renal cell carcinomas on three-phase MDCT: usefulness of the measurement of degree and heterogeneity of enhancement *Acta Radiologica* 2012;53: 112 –118.
11. Kim JK, Kim TK, Ahn HJ, Kim CS, Kim KR, Cho KS. Differentiation of subtypes of renal cell carcinoma on helical CT scans. *AJR Am J Roentgenol*. 2002 Jun;178(6):1499-506.
12. Nightingale K, Soo MS, Nightingale R, Trahey G. Acoustic radiation force impulse imaging: in vivo demonstration of clinical feasibility. *Ultrasound Med Biol*. 2002 Feb;28(2):227-35.

13. D'Onofrio M, Gallotti A, Mucelli RP. Tissue quantification with acoustic radiation force impulse imaging: Measurement repeatability and normal values in the healthy liver. *AJR* 2010;195: 132–136.
14. Fahey BJ, Nelson RC, Bradway DP, Hsu SJ, Dumont DM, Trahey GE. In vivo visualization of abdominal malignancies with acoustic radiation force elastography. *Phys Med Biol*. 2008 Jan 7;53(1):279-93.
15. Pallwein L, Mitterberger M, Struve P, Pinggera G, Horninger W, Bartsch G et al. Real-time elastography for detecting prostate cancer: preliminary experience. *BJU Int*. 2007 Jul;100(1):42-6.
16. Onur MR, Poyraz AK, Ucak EE, Bozgeyik Z, Özercan İH, Ogur E. Semi-quantitative strain elastography of liver masses. *J Ultrasound Med*. 2012;31: 1061-1067.
17. Menzilcioglu MS., Duymus M., Citil S., Avcı S., Gungor G., Sahin T., et al. Strain wave elastography for evaluation of renal parenchyma in chronic kidney disease. *The British Journal of Radiology*, 2015;88(1050), 20140714.
18. Orlacchio A, Chegai F, Del Giudice C, Anselmo A, Iaria G, Palmieri G, et al. Kidney transplant: usefulness of real-time elastography (RTE) in the diagnosis of graft interstitial fibrosis. *Ultrasound Med Biol*. 2014 Nov;40 (11):2564-72.
19. Gao J, Rubin JM. Ultrasound strain zero-crossing elasticity measurement in assessment of renal allograft cortical hardness: a preliminary observation. *Ultrasound Med Biol* 2014;40:2048–57.
20. Ozkan F, Yavuz YC, Inci MF, Altunoluk B, Ozcan N, Yuksel M, et al. Interobserver variability of ultrasound elastography in transplant kidneys: correlations with clinical-Doppler parameters. *Ultrasound Med Biol*. 2013 Jan;39(1):4-9.
21. Duymuş M, Menzilcioğlu MS, Gök M, Avcu S. Kidney Ultrasound Elastography: Review. *Kafkas J Med Sci* 2016; 6(2):121–129.
22. Tan S, Özcan MF, Tezcan F, Balci S, Karaoğlanoğlu M, Huddam B, et al. Real-time elastography for distinguishing angiomyolipoma from renal cell carcinoma: preliminary observations. *AJR Am J Roentgenol*. 2013 Apr;200(4):W369-75.
23. Keskin S, Güven S, Keskin Z, Özbiner H, Kerimoğlu Ü, Yeşildağ A. Strain elastography in the characterization of renal cell carcinoma and angiomyolipoma. Can Urol Assoc J 2015;9(1-2):e67-71.